



ORIGINAL ARTICLE - GASTROENTEROLOGY (EXPERIMENTAL)

Extracellular vesicles produced by bone marrow mesenchymal stem cells overexpressing programmed death-ligand 1 ameliorate dextran sodium sulfate-induced ulcerative colitis in rats by regulating Th17/Treg cell balance through PTEN/PI3K/AKT/mTOR axis

Hongxia He,¹ Qianyun Chen,¹ Heng Fan,¹ Xue yuan Leng,¹ Feng Zhu,¹  Fei Gao, Qiaoli Zhou, Yalan Dong and Jia Yang 

Department of Integrated Traditional Chinese and Western Medicine, Union Hospital, Tongji Medical College, Huazhong University of Science and Technology, Wuhan, 430022, China

Key words

bone marrow-derived mesenchymal stem cells, extracellular vesicles, programmed death-ligand 1, PTEN/PI3K/AKT/mTOR axis, ulcerative colitis.

Accepted for publication 22 August 2022.

Correspondence

Jia Yang, Department of Integrated Traditional Chinese and Western Medicine, Union Hospital, Tongji Medical College, Huazhong University of Science and Technology, Wuhan 430022 China.
Email: 360236862@qq.com¹Hongxia He, Qianyun Chen, and Heng Fan have contributed equally to this work and share first authorship.**Author contribution:** HXH, QYC, and HF carried out most of the research, analyzed the data, and drafted the manuscript. XYL, FZ, FG, QLZ, and YLD co-conducted the study. JY conceived the study and participated in the research design and coordination. All authors read and approved the final manuscript.**Ethical approval:** All the experiments were performed according to guidelines and study protocols of the Institutional Animal Care and Use Committee at Tongji Medical College, Huazhong University of Science and Technology (IACUC number, S1182).

Abstract

Background and Aim: Programmed death-ligand 1 (PD-L1) was involved in regulating Th17/Treg cell balance in ulcerative colitis (UC). Extracellular vesicles (EVs) from genetically modified bone marrow mesenchymal stem cells (BMSCs) can serve as a stable delivery system to overexpress PD-L1. The study was designed to evaluate the therapeutic mechanism of BMSC-EVs overexpressing PD-L1 (PD-L1-EVs) on ulcerative colitis.**Methods:** Experimental model of UC was established in rats by drinking 5% dextran sulfate sodium (DSS). Apoptosis-related proteins, inflammatory response-related factors and oxidative stress related mediators were detected. Westernblot was used to detect key proteins in the PI3K/AKT signaling pathway and its downstream effectors. The CD4⁺Foxp3⁺Treg cells and CD4⁺IL-17A⁺Th17 cells in spleen and mesenteric lymph nodes (MLNs) was detected by flow cytometry.**Results:** PD-L1-EVs significantly alleviated the manifestations and pathological damage of UC rats by inhibiting the expression of IFN- γ , IL-1 β , IL-8, IL-6, IL-2, BAX, NF- κ B, TNF- α , MPO, and MDA, and up-regulating the expression of IL-4, BCL-2, SOD, and GSH. Furthermore, the proportions of Th17 cells were decreased and that of Treg cells were upregulated by PD-L1-EVs treatment. PTEN inhibitors (bpv) partially abolished the inhibitory effect of PD-L1-EVs on PI3K-AKT signaling and impaired the therapeutic efficacy of PD-L1-EVs.**Conclusions:** PD-L1-EVs mitigated colonic inflammation, apoptosis and oxidative stress through blocking the activation of PI3K/Akt/mTOR pathway and regulating the balance of Th17/Treg cells.**Financial support:** This work was supported by National Natural Science Foundation of China (grant number 81904015).

Introduction

Ulcerative colitis (UC) is a relapsing and refractory intestinal non-specific inflammatory disease,¹ belonging to a kind of autoimmune disease. Its typical clinical manifestations includes bloodydiarrhea, abdominal pain, fecal urgency, and tenesmus, while anemia, fatigue and poor appetite as the concomitant symptom are also prevalent.^{2,3} Autoimmune disease features the abnormalities of innate and adaptive immune responses, which also underlies

the pathogenesis of UC.^{4–9} Recent studies have shown that regimens to regulate the Th17/Treg cell balance could suppress autoimmune diseases pathogenesis and progression.^{7–9} Unbalanced intestinal immune homeostasis caused by excessive activation of T cells was one of the important characteristics of UC, which leads to the release of pro-inflammatory mediators, the abnormal aggregation of immune cells and the destruction of intestinal mucosal tissue.¹⁰ Emerging evidence also indicates that UC is caused by excessive activation of Th17 cells or deficiency of Treg cells.^{11,12} Therefore, inhibiting the activation of T lymphocytes and modulating the balance of Th17/Treg cells might be a crucial strategy to hinder the occurrence or development of UC.

The co-inhibitory receptor programmed death 1 (PD-1) and its ligands (PD-L1) are critical regulators in self-tolerance and autoimmunity.^{5,13} Recent studies have shown that PD-1 or PD-L1 knockout can cause a variety of autoimmune diseases, such as systemic lupus erythematosus, rheumatoid arthritis (RA), and type 1 diabetes mellitus.¹⁴ PD-L1 knockout mice were more vulnerable to intestinal injury induced by dextran sodium sulfate (DSS), as is indicated by the high morbidity and mortality. However, administration of adenovirus expressing Fc-conjugated PD-L1 could significantly ameliorate DSS-induced colitis in mice,¹⁵ the mechanism of which may involve the forced interaction between Fc-conjugated PD-L1 and PD-1 and PD-1-mediated inhibitory signals.¹⁶ PD-L1-coated beads could induce Tregs *in vitro*, as Francisco *et al.* reported before, and PD-L1 could increase Foxp3 expression and enhance the immunosuppressive ability of Tregs.¹⁷ Therefore, PD-L1 is able to inhibit T cell response by promoting the induction and maintenance of iTreg cells. Thus, we suggest that delivering PD-L1 may provide a novel therapeutic approach to alleviate intestinal inflammation by maintaining the balance between Treg and Th17 cells.

BMSCs therapy is a cell-based treatment for inflammatory disorders. BMSCs have great immunosuppressive properties which can inhibit T cells activation and alter the phenotype of macrophages and dendritic cells (DCs) in various preclinical and clinical studies.¹⁸ However, the safety of BMSCs remains controversial. Compared with BMSCs, EVs derived from BMSCs feature not only the similar immunoregulatory capacity but also low immunogenicity. Furthermore, they present lower risk of tumor transformation and higher transplantation efficiency in relative to BMSCs.¹⁹ Genetically modified EVs offered a highly-plastic strategy for the treatment of UC.

In this study, we transfected BMSCs with lentivirus to obtain EVs overexpressing PD-L1. The protective effect of PD-L1-EVs on DSS-induced colitis was evaluated and the underlying mechanism was explored.

Materials and methods

Isolation, cultivation, and identification of bone marrow mesenchymal stem cells. Bone marrow mesenchymal stem cells (BMSCs) were isolated from the bone marrow of Sprague–Dawley (SD) rats weighing 60–80 g, and cultured in F12 (Gibco, USA) supplemented with 10% fetal bovine serum (FBS, Gibco, USA), as previously described.¹⁹ The medium was changed every 3 days. Cells at 3th to 4th passage (P3 to P4) were utilized for subsequent experiments.

Construction of recombinant lentivirus and virus infection. The rat PD-L1 gene fragments were acquired through a chemical synthesis method by Shanghai Generay Biotech Co., Ltd. The restriction enzyme BamHI/AgeI were used to digest the lentiviral vector. Recombinant lentiviruses co-expressing anti-purinomycin gene and PD-L1 or siPD-L1 was constructed in 293 T cell lines. Transfection was performed at a multiplicity of infection of 40 in the presence of 100 μ l HitransG P (Genechem) following the manufacturer's instructions.

The generation and identification of extracellular vesicles produced by bone marrow mesenchymal stem cells. The P3–P4 BMSCs, 70% to 80% confluent, were used to extract EVs through ultracentrifugation, as previously reported.²⁰ The morphology of isolated EVs was observed under 200 kV transmission electron microscope (TEM) (HITACHI H-7000FA, Japan). Western blot was used to detect the expression of surface epitopes protein (CD63, TSG101 and PD-L1) in EVs.

Induction of colitis and treatment. Specific-pathogen-free (SPF) male Sprague–Dawley rats were provided by the experimental animal center of Huazhong University of Science and Technology (HUST, Wuhan, China). One week after adaptive feeding, colitis was induced by 5% DSS (MP Biomedicals, Illkirch, France) according to methods described by Ma *et al.*²¹ Animals were randomly divided into eight groups, namely, Control group, DSS group, SiPD-L1-EVs group, PD-L1-EVs group, EVs group, Mesalazine group, PD-L1-EVs + PTEN inhibitor (bpv) group and bpv group. Among them, SiPD-L1-EVs, EVs or PD-L1-EVs were all suspended in PBS and administrated at a dose of 200 μ g/kg by tail vein injection²² on the third day after modeling. PD-L1-EVs + bpv and bpv group were intraperitoneally injected with bpv once a day (0.4 mg/kg/DAY, EMD Chemicals, Inc., NJ, USA) for 5 days from the third day after modeling. The mesalazine group was given mesalazine (0.42 g/kg) intragastric administration for 5 days starting from day 3 of modeling ($n = 10$ for each group). On the day 8, all the animals were anesthetized with 2% sodium pentobarbital and then sacrificed.

Disease activity index score evaluation. The mental state, hair and activity state of rats in each group were observed every day, and the changes of weight, stool and blood in stool of rats were recorded to evaluate Disease activity index (DAI)¹⁹ as in the Table S1.

Histological processing and analysis. The fresh distal colonic tissues of rats were fixed in 4% paraformaldehyde and stained with hematoxylin and eosin (H&E, Jiancheng, Nanjing, China). Histological evaluations of HE-stained colonic sections were graded as Table S2.

Immunohistochemistry and immunofluorescent staining. Fresh colon tissue samples from rats were fixed with 4% paraformaldehyde. Then, 5- μ m-thick sections were embedded in paraffin. The sections were then incubated with anti-BCL-2-(BOSTER), anti-BAX (Abcam), anti-NF- κ B (Abcam), anti-TNF- α (Abcam) primary antibodies overnight at 4°C, followed by

incubation with a biotinylated secondary antibody.^{19,23} We used a light microscope to image the Immunohistochemistry (IHC) slides. For immunofluorescent (IF) staining, dewaxed sections were pre-incubated in PBS containing 3% BSA for 30 minutes. Sections were then counterstained with DAPI, washed, and mounted with anti-fading medium.²⁴ Fluorescence microscope was applied to examine the expression levels of HIF- α (Abcam), FoxO1 (Abcam), p53 (Abcam) and anti-c-caspase 9 (Affinity).

Enzyme-linked immunosorbent assay. The expression levels of IFN- γ , IL-1 β , IL-8, IL-6, IL-4, IL-2, IL-17A, IL-21, IL-10 and TGF- β in the eyeball blood or colon homogenate supernatants of rats were measured using Enzyme-linked immunosorbent assay (ELISA) kits (Elabscience Biotechnology, Wuhan, China) according to the manufacturer's instruction. Briefly, the standard was diluted first, then the samples and the biotin-labeled antibody were added to the antibody-labeled plate. Subsequently, the enzyme was added at 37°C for 30 min. The plate was washed five times with the washing liquid before adding the coloring solution and the stopping liquid. The absorbance was read at 450 nm.

Western blotting. Western blotting (WB) was performed according to the previous description.¹⁹ Generally speaking, extracting the total proteins from colon tissue samples with RIPA lysis buffer mixed with protease inhibitor cocktail (Roche, Basel, Switzerland). To separate proteins, we used Sodium dodecyl sulfate-polyacrylamide gel electrophoresis. Subsequently, the protein was transferred onto a polyvinylidene difluoride membrane which was block with 5%skim milk, and then incubated overnight at 4°C with appropriate primary antibodies against TSG101 (Abcam, 1: 1000), CD63 (Abcam, 1: 1000), PD-L1(Affinity, 1:500), BCL-2(BOSTER, 1:2000), BAX (Abcam, 1:500), NF- κ B (Abcam, 1:2000), TNF- α (Abcam, 1:1000), p-PTEN (Abcam, 1:5000), PD-1 (Proteintech, 1:5000), p-PI3K (Affinity, 1:1000), p-AKT (CST, 1:2000), p-mTOR (Affinity, 1:500), HIF- α (Abcam, 1:500), FoxO1 (Abcam, 1:1000), p53 (Abcam, 1:2000) and c-caspase 9 (Affinity, 1:1000). In the end, TBST was used to wash the membrane, and then the second antibody (HRP-Goat anti Rabbit, Elabscience, 1:3000; or HRP-Goat anti Mouse, Elabscience,1:3000) was added and incubated for 1 h at room

temperature. The protein expression was normalized to β -actin or GAPDH.

Quantitative real-time PCR analysis. According to the manufactures' instructions, total RNA from colon samples was extracted with Trizol reagent (Solarbio, Beijing, China). The cDNA was then obtained using reverse transcribe PrimeScript 1st Strand cDNA synthesis kit (TAKARA, Kyoto, Japan). Finally, real-time reverse-transcription polymerase chain reaction was carried out. Forward and reverse primers of related genes were as shown in Table S3. The relative expression of the target genes was calculated by the delta-delta Ct method, also referred to as the $2^{-\Delta\Delta Ct}$ method²⁵ with normalization to β -actin mRNA.

Biochemical detection. The activities of myeloperoxidase (MPO), superoxide dismutase (SOD) and the concentration of glutathione (GSH), malondialdehyde (MDA) in the colon were detected using the commercial assay kit (Jiancheng Bioengineering Institute, Nanjing, China) according to the manufacturer's instruction.

Flow cytometry. Mononuclear cells were isolated from spleen and MLNs as described previously.²⁶ Th17 and Treg cells were stained as described by Yu *et al.*²⁰ BD GolgiPlug™ (BD Biosciences), FITC-anti-CD45 antibody and PE-Cy7-anti-CD4 antibody (BD Biosciences, San Diego, CA, USA), eFluor 450-anti-IL-17A antibody (eBioscience, San Diego, CA, USA), and PE-anti-Foxp3 antibody (eBioscience, San Diego, CA, USA) were used.

Statistical analyses. We performed the statistical analyses with SPSS 25.0 software. The two-tailed student's t test was applied for the statistical comparison between two groups, and one-way ANOVA was used for three or more sets of data. $P < 0.05$ was considered statistically significant.

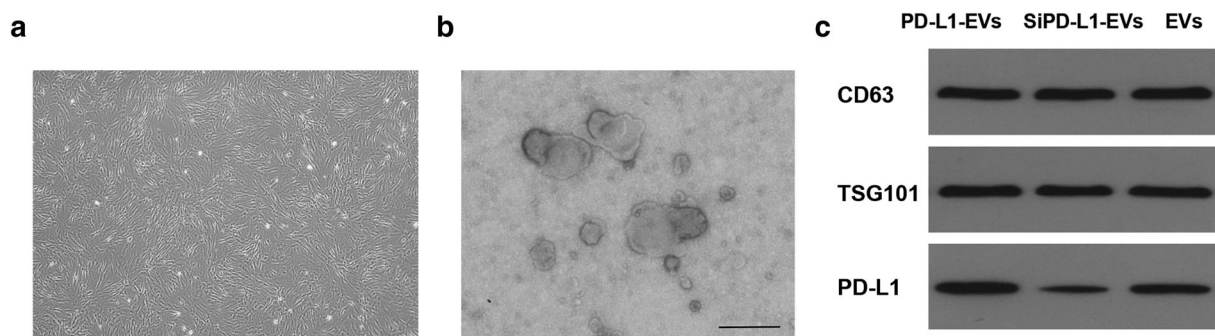


Figure 1 Characterization of BMSCs and PD-L1-EVs. (a) Representative image of P4 BMSCs. Original magnification, 40 \times . (b) Transmission electron microscopy (TEM) analysis of EVs derived from BMSCs. Scale bar, 200 nm. (c) Western blotting analysis of proteins TSG101, CD63, and PD-L1 in gene-modified EVs.

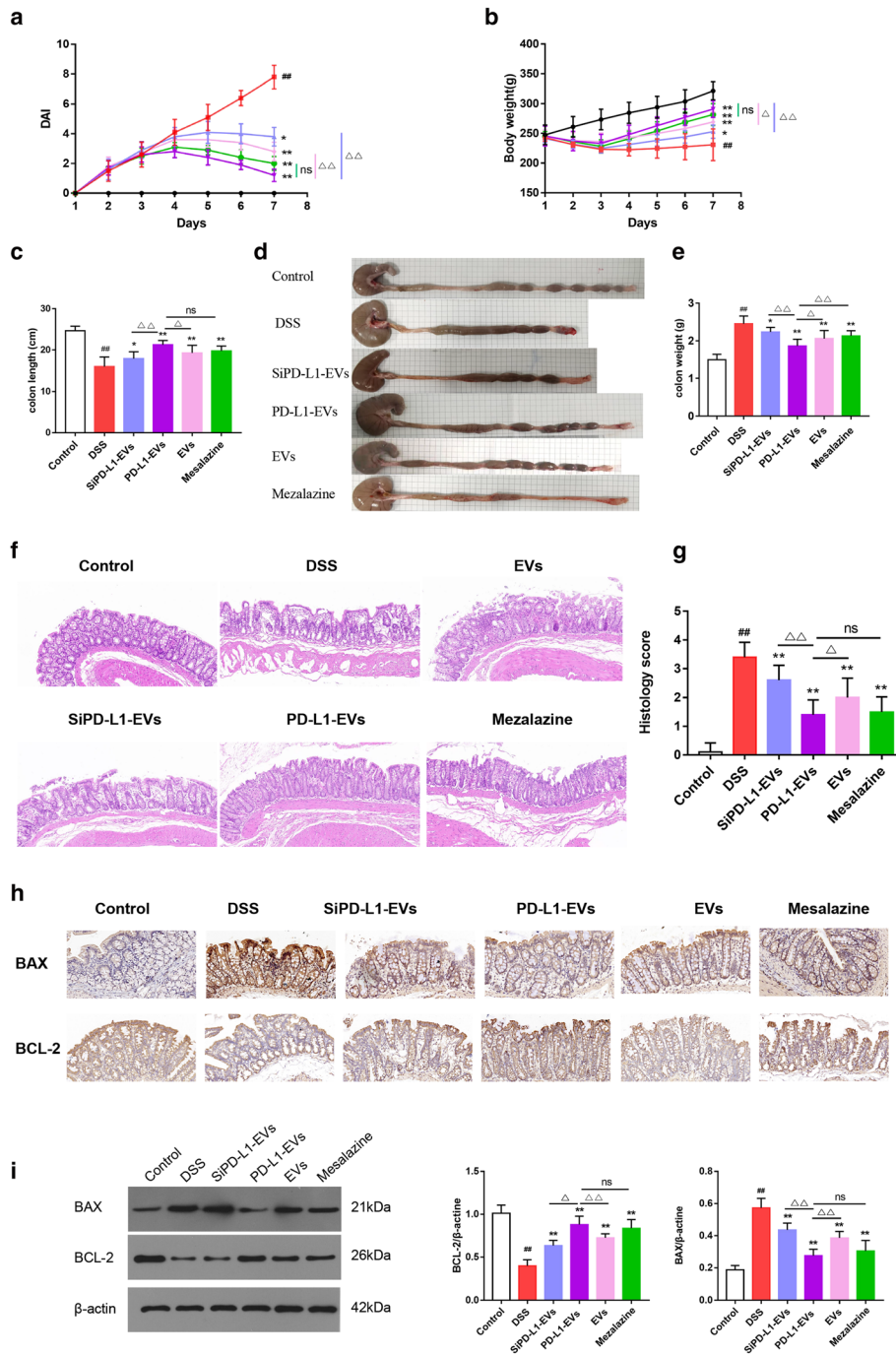


Figure 2 PD-L1-EVS' alleviation on colitis damages. (a) DAI score. (b) Body weight. (c) Colon length. (d) Representative picture of colons. (e) Colon weight. (f) Hematoxylin and eosin (HE) staining of colon tissue. Original magnification, 200 \times . (g) Histopathological score based on HE staining. (h) Immunohistochemical staining for BCL-2, BAX in colon tissue. Original magnification, 200 \times . (i) Western blotting analysis of proteins BCL-2 and BAX in colon tissue. β -actin was used as a loading control. (# $P < 0.05$, ## $P < 0.01$, DSS group vs Control group; * $P < 0.05$, ** $P < 0.01$, each treatment group vs DSS group; $\Delta P < 0.05$, $\Delta\Delta P < 0.01$, vs PD-L1-EVs group). (a, b) \blackrightarrow , Control; $\color{red}\blackrightarrow$, DSS; $\color{blue}\blackrightarrow$, SiPD-L1-EVs; $\color{purple}\blackrightarrow$, PD-L1-EVs; $\color{pink}\blackrightarrow$, EVs; $\color{green}\blackrightarrow$, Mesalazine.

Results

Characterization of rat gene-modified bone marrow mesenchymal stem cells and extracellular vesicles. Microscopically, BMSCs appear as spindle cells in a swirling pattern (Fig. 1a). The expression of CD29, CD90,

CD11b, and CD45 in BMSCs were also validated by flow cytometry.¹⁹ Under TEM, EVs were typically spherical and the diameter fluctuated between 30 and 200 nm (Fig. 1b). The expression of EVs markers CD63 and TSG101 in PD-L1-EVs group, SiPD-L1-EVs group and EVs group were detected by western blotting. The result showed that the PD-L1 level in PD-L1-EVs

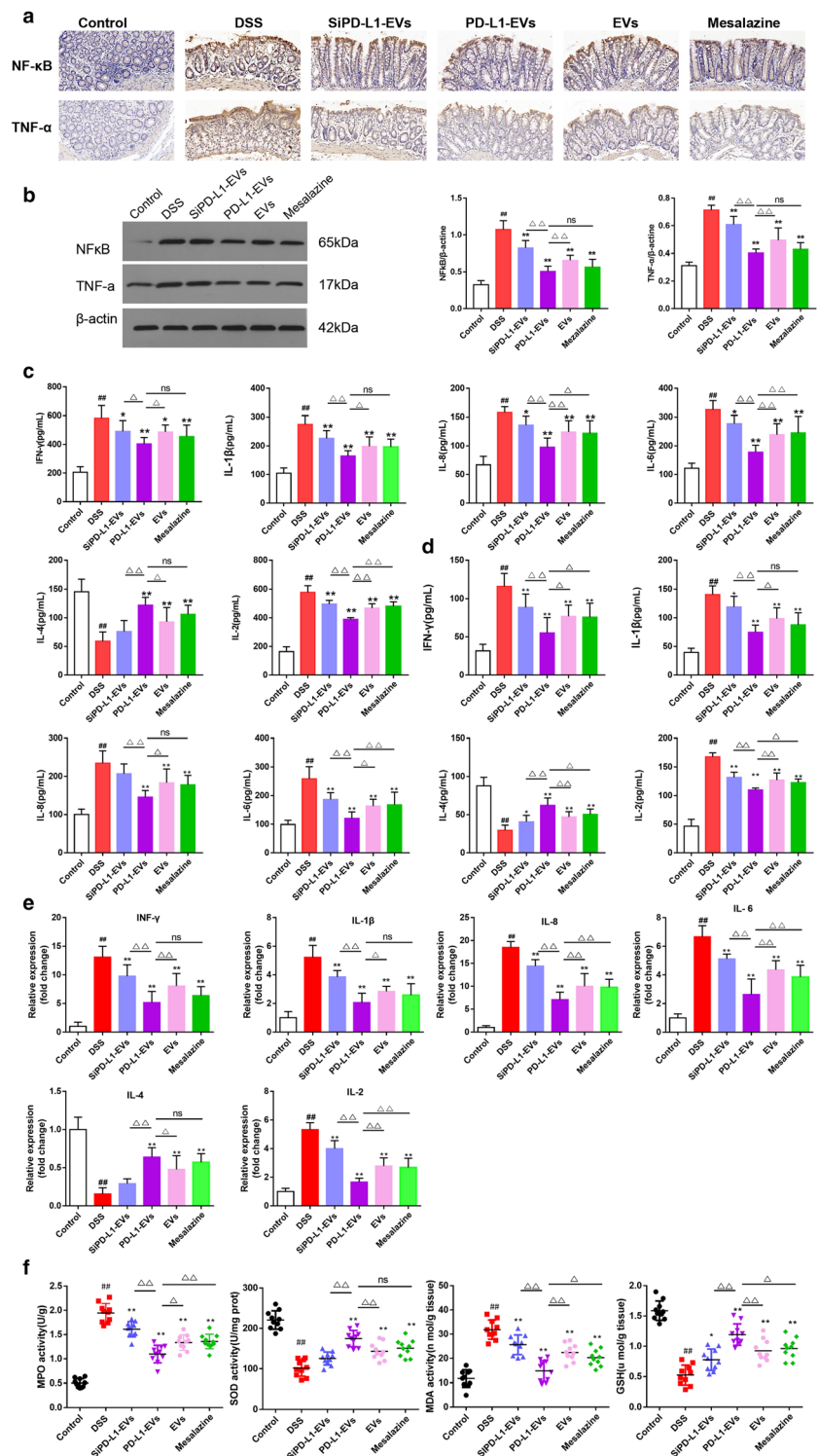


Figure 3 PD-L1-EVs suppress the production of inflammatory mediators and alleviate DSS-induced oxidative stress in colitis rats. (a) Immunohistochemical staining for NF-κB and TNF-α in colon tissue. Original magnification, 200x. (b) Western blotting analysis of NF-κB and TNF-α in colon tissues. β-actin was used as a loading control. (c) The concentrations of IFN-γ, IL-1β, IL-8, IL-6, IL-4 and IL-2 in colon tissue were detected by ELISA. (d) The concentrations of IFN-γ, IL-1β, IL-8, IL-6, IL-4, and IL-2 in serum were detected by ELISA. (e) Relative expression of IFN-γ, IL-1β, IL-8, IL-6, IL-4, and IL-2 in colons tissue was detected by qRT-PCR. (f) Expression levels of MPO, SOD, MDA, and GSH in colon tissue. (#*P* < 0.05, ###*P* < 0.01, DSS group vs Control group; **P* < 0.05, ***P* < 0.01, each treatment group vs DSS group; Δ*P* < 0.05, ΔΔ*P* < 0.01, vs PD-L1-EVs group).

group was significantly higher than in SiPD-L1-EVs and EVs group (Fig. 1c).

PD-L1-EVs significantly attenuated the severity of dextran sodium sulfate-induced colitis in rats.

DAI score in DSS group increased along the modeling, manifested by severe diarrhea, bloody stools, and weight loss. However, animals treated with PD-L1-EVs and mesalazine showed significantly reduced DAI score compared with the DSS group (Fig. 2a, $**P < 0.01$). Model rats suffered significant body weight loss, while the treatment of PD-L1-EVs and mesalazine dramatically reversed the trend of weight loss (Fig. 2b, $**P < 0.01$). In addition, colon length shortening and colon weight gain, key features of inflammatory colon injury, were markedly reversed with the intervention of PD-L1-EVs and mesalazine compared with the DSS group (Fig. 2c–e, $**P < 0.01$). The severity of colitis was further assessed by histopathological analysis. A series of pathological changes such as disturbed mucosal structure, glandular destruction, tissue edema and inflammatory cell infiltration were observed in the DSS group (Fig. 2f). Nevertheless, PD-L1-EVs and mesalazine exhibited obvious protection in regards to mucosa injury and histological inflammation, indicated by lower histopathological score (Fig. 2g, $**P < 0.01$). Moreover, compared with the SiPD-L1-EVs and EVs group, the severity of colitis in PD-L1-EVs group was significantly reduced ($\Delta P < 0.05$).

PD-L1-EVs could regulate the expression of apoptosis-related proteins in colon tissues of ulcerative colitis rats.

The effects of PD-L1-EVs on BAX and BCL-2 in colon tissue were detected by immunohistochemical analysis and WB. Compared with DSS group (0.573 ± 0.057 ; 0.399 ± 0.067), BAX was down-regulated while BCL-2 up-regulated in PD-L1-EVs (0.276 ± 0.038 ; 0.881 ± 0.091) and mesalazine group (0.305 ± 0.062 ; 0.836 ± 0.096) (Fig. 2h,i, $**P < 0.01$). Compared with the SiPD-L1-EVs and EVs, PD-L1-EVs had a stronger ability to regulate the expression of apoptosis-related proteins in UC rat colon tissue ($\Delta P < 0.05$).

PD-L1-EVs attenuated dextran sodium sulfate induced inflammation response and oxidative stress.

As shown in the picture below (Fig. 3a,b), compared with DSS group (1.073 ± 0.114 ; 0.715 ± 0.032), NF- κ B and TNF- α proteins were significantly decreased in PD-L1-EVs (0.508 ± 0.067 ; 0.403 ± 0.027) and mesalazine group (0.566 ± 0.101 ; 0.430 ± 0.045) ($**P < 0.01$). The concentrations of pro-inflammatory cytokines IFN- γ , IL-1 β , IL-8, IL-6 and IL-2 in PD-L1-EVs (IFN- γ : 403.482 ± 42.540 ; IL-1 β : 164.605 ± 17.760 ; IL-8: 97.616 ± 15.198 ; IL-6: 178.091 ± 22.887 ; IL-2: 389.788 ± 10.924 ; IL-4: 121.879 ± 13.098) and mesalazine group (IFN- γ : 455.343 ± 75.672 ; IL-1 β : 196.648 ± 29.816 ; IL-8: 121.882 ± 20.736 ; IL-6: 245.034 ± 54.758 ; IL-2: 480.087 ± 29.687 ; IL-4: 106.006 ± 15.163) were significantly decreased, and the concentrations of anti-inflammatory factors IL-4 were significantly increased, compared with DSS group (IFN- γ : 583.500 ± 81.438 ; IL-1 β : 275.306 ± 28.477 ; IL-8: 158.013 ± 9.606 ; IL-6: 326.307 ± 29.375 ; IL-2:

578.310 ± 43.862 ; IL-4: 59.294 ± 15.187) (Fig. 3c, $**P < 0.01$). The trend of these inflammatory factors in serum was roughly consistent with that in colon tissue (Fig. 3d, $**P < 0.01$). Relative expression of IFN- γ , IL-1 β , IL-8, IL-6, IL-4, and IL-2 in colons tissue was detected by quantitative real-time PCR analysis (qRT-PCR). The results of mRNA were consistent with the expression trend of the corresponding proteins (Fig. 3e, $**P < 0.01$). MPO, MDA, GSH and SOD are known to be involved in oxidative stress and inflammatory response.²⁰ Animals treated with DSS exhibited increased activity of MPO (1.944 ± 0.186), elevated MDA (31.861 ± 3.759), and decreased SOD (101.880 ± 19.285) and GSH (0.526 ± 0.156) (Fig. 3f, $##P < 0.01$). Compared with the DSS group, PD-L1-EVs (1.098 ± 0.171 ; 14.853 ± 4.087 ; 174.786 ± 19.151 ; 1.193 ± 0.168) and mesalazine (1.357 ± 0.142 ; 20.296 ± 3.281 ; 150.842 ± 19.913 ; 0.962 ± 0.162) group showed much less abnormality in the levels of MPO, MDA, SOD, and GSH (Fig. 3f, $**P < 0.01$).

PD-L1-EVs blocked the activation of PI3K/Akt/mTOR pathway in dextran sodium sulfate-induced colitis in rats.

In order to further explore the mechanism of PD-L1-EVs, PTEN inhibitor, bpv, was used to further confirm our hypothesis that PTEN/PI3K/AKT/mTOR pathway is an important signal pathway downstream of PD-L1. HE staining showed that after the treatment of PD-L1-EVs, a series of pathological changes such as mucosal structure disorder, gland destruction, tissue edema and inflammatory cell infiltration induced by DSS were alleviated (Fig. 4a). At the same time, histopathological scores were reduced and the weight loss was effectively reversed (Fig. 4b,c, $**P < 0.01$). However, with the intervention of bpv, these beneficial effects of PD-L1-EVs on UC rats were attenuated ($\Delta\Delta P < 0.01$). WB was used to detect the protein expression levels of PD1, p-PTEN, PD-L1, p-PI3K, p-AKT, and p-mTOR (Fig. 4d). We found that drinking water with 5% DSS dramatically elevated the phosphorylation of PI3K, Akt and mTOR in colon tissue, whereas this abnormal elevation could be reversed by treatment with PD-L1-EVs (Fig. 4e, $**P < 0.01$). These changes partly abolished by bpv (Fig. 4e, $\Delta\Delta P < 0.01$). Therefore, the results indicated that PD-L1-EVs could block the activation of PI3K/Akt/mTOR pathway in DSS-induced colitis in rats. Next, we further explored some molecular expressions downstream of this pathway. WB strip results displayed that bpv intervention attenuated the effect of PD-L1-EVs in regulating expression level of HIF- α , p53, c-caspase 9, and FoxO1 (Fig. 5a,b, $\Delta\Delta P < 0.01$). Similarly, immunofluorescence staining showed the same trend (Fig. 5c,d).

PD-L1-EVs regulated the balance of Th17/Treg cell in colitis rats through PTEN/PI3K/AKT/mTOR pathway.

The effects of PD-L1-EVs on Th17 and Treg cells differentiation were investigated by flow cytometry. Compared with the DSS group, CD4⁺Foxp3⁺Treg cells in spleen and MLNs in PD-L1-EVs group were significantly increased, and CD4⁺IL-17A⁺Th17 cells were significantly decreased (Fig. 6a–f, $**P < 0.01$). DSS-induced colitis rats exhibited upregulation of IL-17A (265.758 ± 20.613) and IL-21 (389.006 ± 49.180) and downregulation of IL-10 (51.845 ± 8.978) and TGF- β (189.330 ± 24.982) in the colonic tissue (Fig. 6g, $##P < 0.01$).

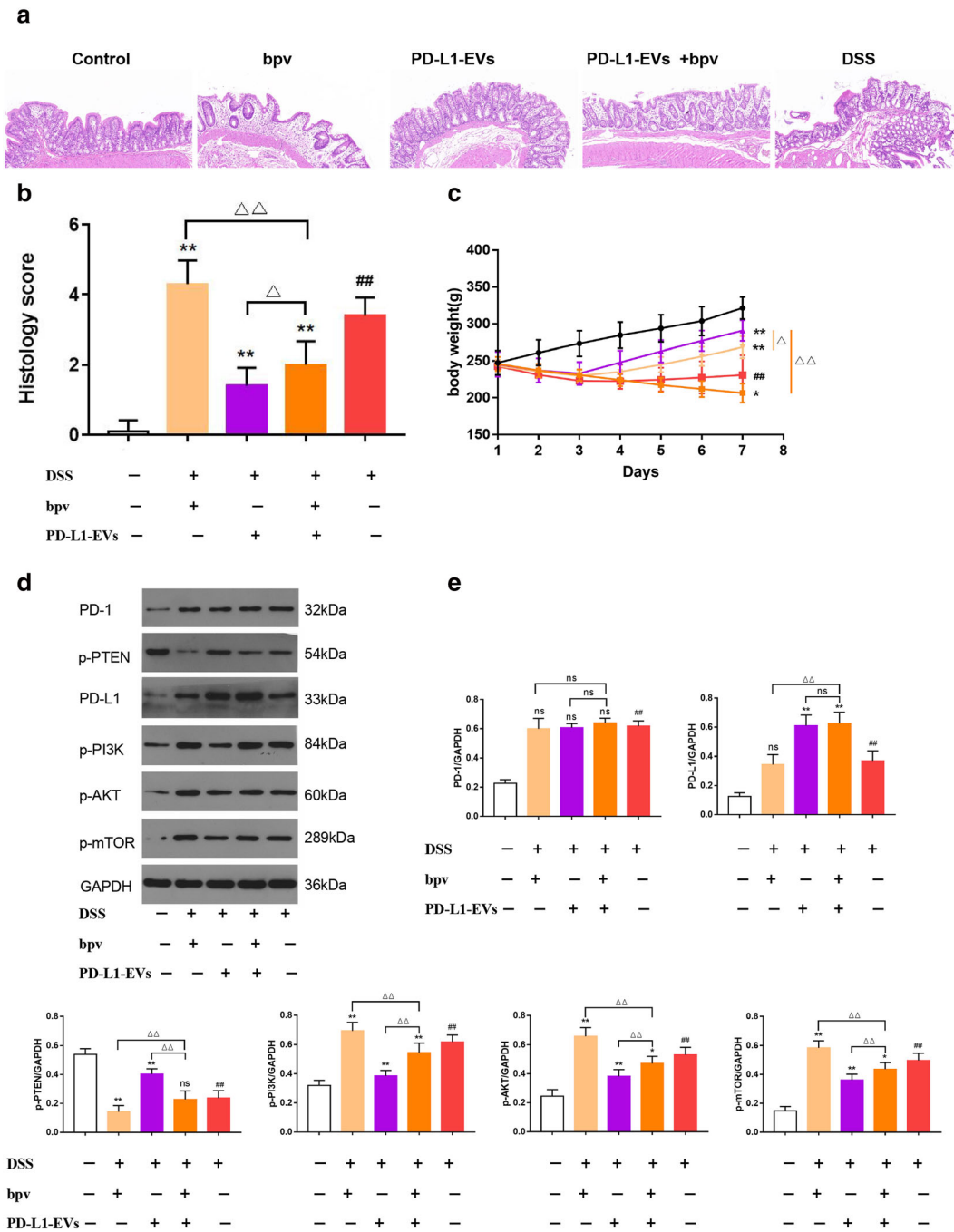


Figure 4 PD-L1-EVs alleviated colitis induced by 5% DSS in rats and regulate the expression of PI3K/Akt/mTOR pathway. (a) Histopathological changes in colon tissues analyzed by hematoxylin and eosin (HE) staining. Original magnification, 100x. (b) Histopathological score of colon sections of rats in each group. (c) The body weight of the rats in each group. (d) Western blotting analysis of PD1, p-PTEN, PD-L1, p-PI3K, p-AKT, and p-mTOR in colon tissue. GAPDH was used as a loading control. (e) The protein quantitative analysis of PD1, p-PTEN, PD-L1, p-PI3K, p-AKT and p-mTOR in colon tissue.###P < 0.01, DSS group vs Control group; *P < 0.05, **P < 0.01, each treatment group vs DSS group; ns: not statistically significant, ΔP < 0.05, ΔΔP < 0.01, vs PD-L1-EVs+bpv group). (c) —, Control; —, bpv; —, PD-L1-EVs; —, PD-L1-EVs+bpv; —, DSS

Treatment with PD-L1-EVs significantly reversed the changes of the above cytokines (194.945 ± 21.434; 289.626 ± 45.083; 70.835 ± 8.992; 328.655 ± 25.780) (Fig. 6g, **P < 0.01). The trend of these signature cytokines in serum was roughly consistent

with that in colon tissue (Fig. 6h, **P < 0.01). Consistently, the mRNA expression of the *IL-17A* and *IL-21* (10.182 ± 1.045; 5.369 ± 0.632) increased, while *IL-10* and *TGF-β* (0.389 ± 0.133; 0.327 ± 0.089) slightly decreased in DSS group

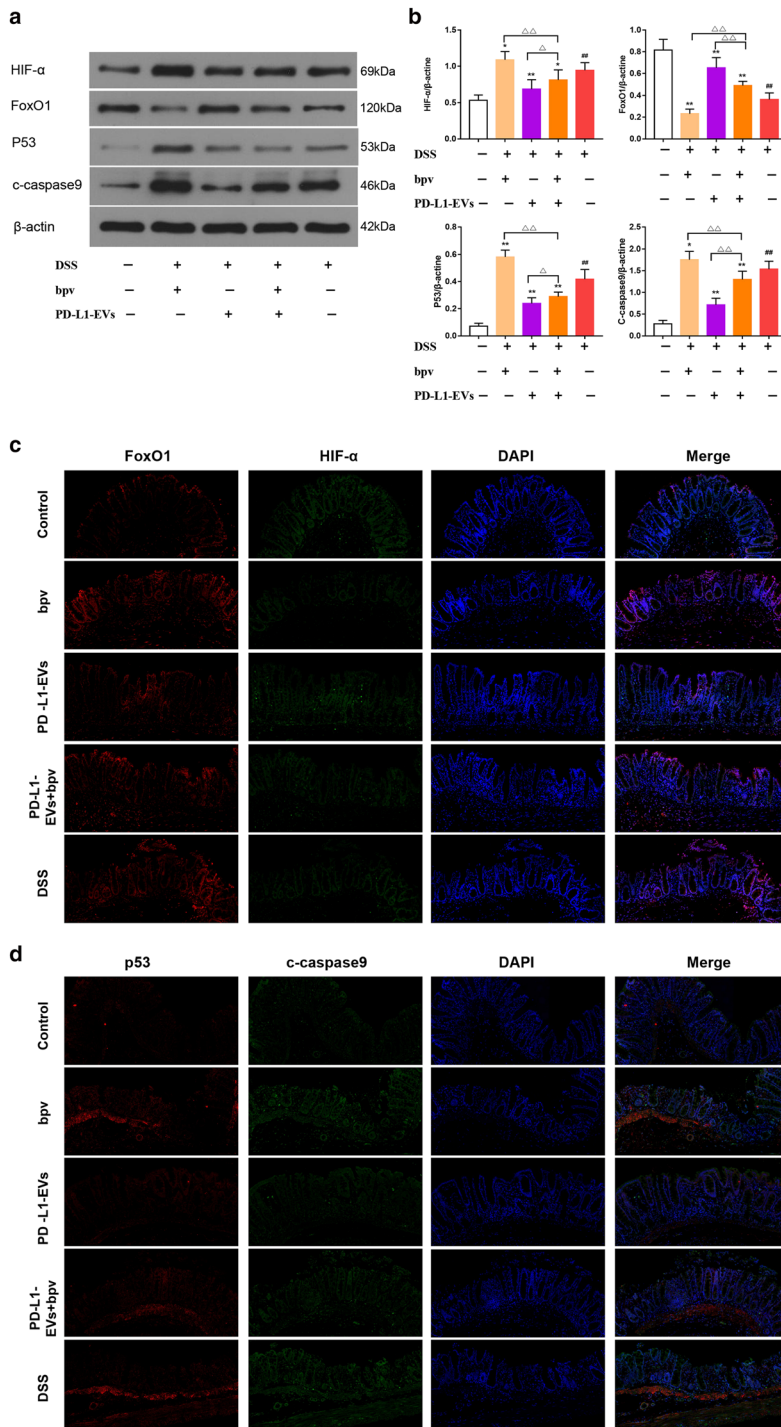


Figure 5 The related proteins of PI3K/Akt/mTOR pathway were regulated by PD-L1-EVs. (a) Western blotting analysis of HIF-α, FoxO1, p53 and c-caspase 9 in colon tissue. β-actin was used as a loading control. (b) The protein quantitative analysis of HIF-α, FoxO1, p53, and c-caspase 9 in colon tissue. (c) Colon tissue were stained with FoxO1 (red), HIF-α (green) and nuclei-stained with DAPI (blue). Fluorescence images were captured using a fluorescence microscope (200×). (d) Colon tissues were stained with p53 (red), c-caspase 9 (green), and nuclei-stained with DAPI (blue). Fluorescence images were captured using a fluorescence microscope (200×). (##*P* < 0.01, DSS group vs Control group; **P* < 0.05, ***P* < 0.01, each treatment group vs DSS group; ns, not statistically significant, Δ*P* < 0.05, ΔΔ*P* < 0.01, vs PD-L1-EVs+bpv group).

(Fig. 6i, ##*P* < 0.01). Treatment with PD-L1-EVs significantly reversed the mRNA expression of these transcription factors (5.162 ± 1.380 ; 2.775 ± 0.262 ; 0.643 ± 0.066 ; 0.643 ± 0.099) (Fig. 6i, ****P* < 0.01). Furthermore, intervention with bpv attenuated the reduction in CD4⁺IL-17⁺Th17 cells and pro-inflammatory cytokines including IL-17A and IL-21 (6.842 ± 1.604 ; 4.389 ± 0.622), and the increment in CD4⁺Foxp3⁺Treg cells and anti-inflammatory cytokine s

including IL-10 and TGF-β (0.530 ± 0.052 ; 0.465 ± 0.104) in the colon tissue in PD-L1-EVs treated colitis rats (Fig. 6a–i, Δ*P* < 0.05).

Discussion

In this study, BMSC-EVs, as the alternative of BMSCs, were used as a carrier to deliver the PD-L1 to the native T cell of UC rats,

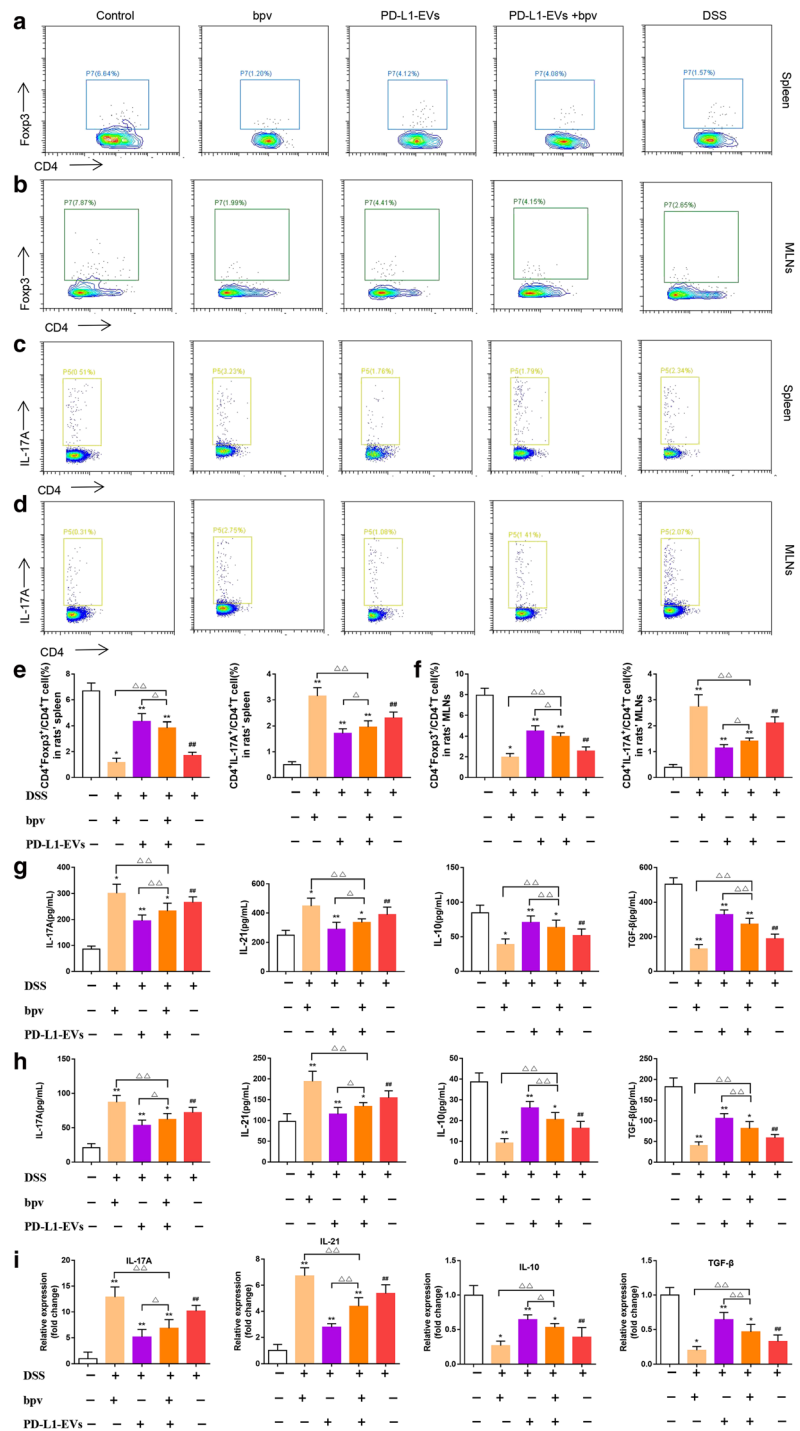


Figure 6 PD-L1-EVs regulated the balance of Th17/Treg cell in colitis rats. (a) The representative FACS plots and the percentages of CD4⁺Foxp3⁺Treg cells in spleen were analyzed by flow cytometry. (b) The representative FACS plots and the percentages of CD4⁺Foxp3⁺Treg cells in MLNs were analyzed by flow cytometry. (c) The representative FACS plots and the percentages of CD4⁺IL-17⁺Th17 cells in spleen were analyzed by flow cytometry. (d) The representative FACS plots and the percentages of CD4⁺IL-17⁺Th17 cells in MLNs were analyzed by flow cytometry. (e) The percentages of CD4⁺Foxp3⁺Treg cells and CD4⁺IL-17A⁺Treg cells in spleen. (f) The percentages of CD4⁺Foxp3⁺Treg cells and CD4⁺IL-17A⁺Treg cells in MLNs. (g) ELISA analysis of IL-17A, IL-21, IL-10, and TGF-β levels in colons. (h) ELISA analysis of IL-17A, IL-21, IL-10, and TGF-β levels in serum. (i) qRT-PCR analysis of IL-17A, IL-21, IL-10, and TGF-β mRNA expression in colons. The expression level of the mRNA was normalized to β-actin. (###*P* < 0.01, DSS group vs Control group; **P* < 0.05, ***P* < 0.01, each treatment group vs DSS group; ns, not statistically significant, Δ*P* < 0.05, ΔΔ*P* < 0.01, vs PD-L1-EVs+bpv group).

which could inhibit the signal transduction of T cells and induce immune tolerance. Compared with SiPD-L1-EVs and EVs group, administration of PD-L1-EVs reduced pathological damage, tissue edema, inflammasome aggregation, and promoted gland integrity in DSS-induced colitis model. These results confirmed that PD-L1-EVs plays an important protective role in the pathological process of UC.

The imbalance between anti-inflammatory and pro-inflammatory cytokines deteriorates UC progression and induced a hyperreactive state.¹⁰ Excessive inflammation is the factor driving the occurrence and development of UC, and also accounts for its pathological characteristics.^{27–29} Th1 differentiation and abnormal activation lead to subsequent IFN-γ production, which is one of the major factors in the progression of UC. Serum levels

of pro-inflammatory cytokines, such as IFN- γ , IL-17, IL-2, TNF- α , IL-1 β , and IL-6, were significantly increased in UC patients.³⁰ Intervention of DSS induced UC rat model by tail vein injection of PD-L1-EVs could significantly reduce the concentration of pro-inflammatory cytokines IFN- γ , IL-1 β , IL-8, IL-6, and IL-2 in colon tissue and serum, and increase the concentration of anti-inflammatory factor IL-4. These results confirmed that PD-L1-EVs could inhibit intestinal inflammatory response and alleviate the development of UC.

As important as inflammatory response, oxidative stress is involved in the pathological process of inflammatory bowel disease.³¹ Massive inflammatory factors release disrupted the balance of oxidants and antioxidants.³¹ In turn, the oxidative stress further exacerbated the inflammatory response.^{32,33} We observed that after treatment with PD-L1-EVs, the MPO activity and MDA expression were significantly decreased in DSS-induced colitis, while the activity of SOD and GSH level were remarkably increased. These results indicated that PD-L1-EVs effectively reduced the oxidative stress.

Apoptotic signaling may promote inflammatory processes by releasing chemokines that may recruit and activate immune cells.³⁴ As reported, mice with elevated apoptosis in their intestinal epithelial cells are more likely to develop intestinal inflammation.³⁴ UC epithelial cell apoptosis is significantly increased, which is thought to be associated with impaired intestinal barrier function.³⁵ Reducing colonic epithelial cell apoptosis is an important strategy in UC therapy. When PD-L1-EVs were administered, compared with DSS group, we found that BAX, p53 and c-caspase 9 was significantly decreased but BCL-2 increased, which indicated that PD-L1-EVs antagonized the processes and proteins in colonic cell apoptosis induced by UC.

As the results above, it was demonstrated that PD-L1-EVs ameliorated inflammation, apoptosis, and oxidative stress during the development of colitis, initiated immune tolerance and inhibited intestinal inflammation. But in fact, the molecular mechanism of PD-L1-EVs is still unclear. Phosphatase and tensin homolog deleted on chromosome 10 (PTEN) negatively regulates the PI3K/AKT signaling pathway.³⁶ To determine whether PD-1/PD-L1 binding restrained the PTEN/PI3K/AKT pathways in UC, colitis rats were treated with bpv (PTEN inhibitor), and the key protein expression of PI3K/AKT/mTOR pathway and its downstream effectors were analyzed by Western blot. Our study indicated that DSS-induced colitis was significantly correlated with the activation of PI3K/AKT/mTOR signaling pathway. The PD-L1-EVs blocked the activation of PI3K/Akt/mTOR pathway by increasing PTEN activity, and that the inhibition of PTEN lead to the activation of PI3K/Akt/mTOR pathway. Meanwhile, this series of events results in changes of HIF- α , FoxO1, p53 and c-caspase 9, downstream in PI3K/AKT/mTOR pathway. Inflammatory cell infiltration could lead to decreased mucosal perfusion in inflamed mucosal tissues, and thus could activate hypoxia-inducible factor 1-alpha (HIF-1 α).^{37,38} Additionally, as a novel target protein, FoxO1 has been reported to negatively regulate the development of UC.³⁹ PI3K/AKT/mTOR signaling pathway negatively regulates FoxP3 expression by inhibiting the activation of the transcription factor Forkhead O3a (FoxO1, 3a).⁴⁰ P53 and c-caspase9 protein are responsible for the regulation of cell cycle and apoptosis, which has a notably higher expression in UC than in normal tissue samples. High expression of p53 and c-caspase9 may indicate increased risk of dysplasia and colorectal cancer (CRC) in UC. The results indicated that the PI3K/AKT/mTOR pathway and its downstream effectors could be regulated by PD-L1-EVs treatment.

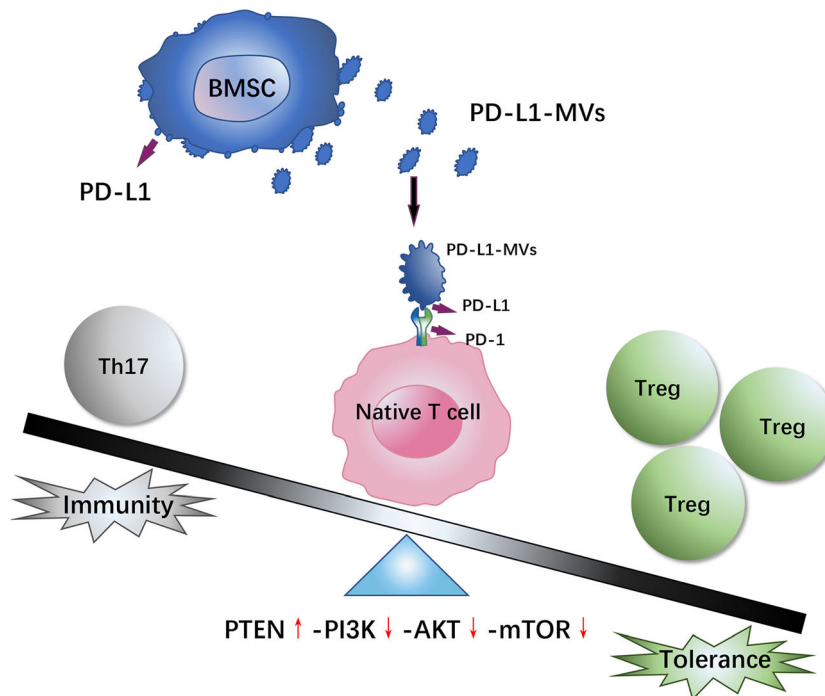


Figure 7 Schematic depiction about the therapeutic effects of PD-L1-EVs.

Th17 cells secrete IL-17A and IL-21, pro-inflammatory cytokines that have been linked to the pathogenesis of autoimmune diseases and to immune responses against bacterial and fungal infections.⁴¹ In contrast, Tregs exert anti-inflammatory functions via the production of cytokines, such as IL-10 and TGF- β , and express inhibitory molecules that suppress pathogenic T cells.^{42–44} An imbalance in the development and function of Th17 and Treg cells plays an important role in several autoimmune and inflammatory diseases,⁴⁵ including UC. Thus, there is a critical need to regulate homeostasis between Treg and Th17 cells. By decreasing Th17 cell response and increasing regulatory T cell responses, the development of autoimmune diseases could be substantially ameliorated.^{46–50} Flow cytometry results showed that injection of PD-L1-EVs could increase the proportion of Treg cells in spleen and MLNs of UC rats, and reduce the proportion of Th17 cells, regulating the proportion of Th17 and Treg cells *in vivo*. These were consistent with dramatic decrease in Th17-related *IL-17A* and *IL-21*, and increase in the Treg-related IL-10 and TGF- β expression. Compared with PD-L1-EVs group, the fluctuation range of the proportion of Th17 cells, IL-17 and IL-21's reduction, and the proportion of Treg cells, IL-10 and TGF- β 's increment in PD-L1-EVs + bpv group was reduced. The underlying mechanism may be that by binding to PD-1 on native T cell, PD-L1-EVs activated immunosuppressive signals PETN/PI3K/AKT/mTOR pathway and regulated the balance of Th17 and Treg, thus maintaining immune tolerance, and alleviating ulcerative colitis (Fig. 7).

In summary, PD-L1-EVs mitigated colon inflammation, apoptosis and oxidative stress through blocking the activation of PI3K/Akt/mTOR pathway and regulating the balance of Th17/Treg cells. Our findings provided insight into the immunobiology of PD-L1-EVs and suggest a useful novel approach to UC treatment. Nevertheless, there remains a limitation in our study. PD1/PD-L1 is an important regulatory pathway of anti-tumor immunity, and anti-PD-1 can produce effective anti-tumor immune activity. If this system is inappropriately stimulated or enhanced, it may increase the possibility of tumorigenesis. To better solve this problem and avoid adverse reactions as much as possible, further exploration is warranted in the future.

Acknowledgments

We are grateful to the Central Laboratory of Wuhan Union Hospital for its instrumental support.

References

- Abraham C, Cho JH. Inflammatory bowel disease. *N. Engl. J. Med.* 2009; **361**: 2066–78.
- Feuerstein JD, Moss AC, Farraye FA. Ulcerative Colitis. *Mayo Clin. Proc.* 2019; **94**: 1357–73.
- Bonne-Année S, Bush MC, Nutman TB. Differential Modulation of Human Innate Lymphoid Cell (ILC) Subsets by IL-10 and TGF- β . *Sci. Rep.* 2019; **9**: 14305.
- Simeone E, Grimaldi AM, Ascierto PA. Anti-PD1 and anti-PD-L1 in the treatment of metastatic melanoma. *Melanoma Manag.* 2015; **2**: 41–50.
- Jiang X, Wang J, Deng X *et al.* Role of the tumor microenvironment in PD-L1/PD-1-mediated tumor immune escape. *Mol. Cancer* 2019; **18**: 10.
- Angelotti F, Parma A, Cafaro G, Capecci R, Alunno A, Puxeddu I. One year in review 2017: pathogenesis of rheumatoid arthritis. *Clin. Exp. Rheumatol.* 2017; **35**: 368–78.
- Nadeem A, Ahmad SF, Attia SM, al-Ayadhi LY, Bakheet SA, al-Harbi NO. Oxidative and inflammatory mediators are upregulated in neutrophils of autistic children: Role of IL-17A receptor signaling. *Prog. Neuropsychopharmacol. Biol. Psychiatry* 2019; **90**: 204–11.
- Bakheet SA, Ansari MA, Nadeem A *et al.* CXCR3 antagonist AMG487 suppresses rheumatoid arthritis pathogenesis and progression by shifting the Th17/Treg cell balance. *Cell. Signal.* 2019; **64**: 109395.
- Ahmad SF, Zoheir KM, Abdel-Hamied HE *et al.* Role of a histamine 4 receptor as an anti-inflammatory target in carrageenan-induced pleurisy in mice. *Immunology* 2014; **142**: 374–83.
- Chen ML, Sundrud MS. Cytokine Networks and T-Cell Subsets in Inflammatory Bowel Diseases. *Inflamm. Bowel Dis.* 2016; **22**: 1157–67.
- Britton GJ, Contijoch EJ, Mogno I *et al.* Microbiotas from Humans with Inflammatory Bowel Disease Alter the Balance of Gut Th17 and ROR γ (+) Regulatory T Cells and Exacerbate Colitis in Mice. *Immunity* 2019; **50**: 212–4.e4.
- Zhang W, Cheng C, Han Q *et al.* Flos *Abelmoschus manihot* extract attenuates DSS-induced colitis by regulating gut microbiota and Th17/Treg balance. *Biomed. Pharmacother.* 2019; **117**: 109162.
- Cai J, Wang D, Zhang G, Guo X. The Role Of PD-1/PD-L1 Axis In Treg Development And Function: Implications For Cancer Immunotherapy. *Onco. Targets. Ther.* 2019; **12**: 8437.
- Sun C, Mezzadra R, Schumacher TN. Regulation and Function of the PD-L1 Checkpoint. *Immunity* 2018; **48**: 434–52.
- Song M-Y, Hong C-P, Park SJ *et al.* Protective effects of Fc-fused PD-L1 on two different animal models of colitis. *Gut* 2015; **64**: 260.
- Boussiotis VA. Molecular and Biochemical Aspects of the PD-1 Checkpoint Pathway. *N. Engl. J. Med.* 2016; **375**: 1767–78.
- Francisco LM, Salinas VH, Brown KE, Vanguri VK, Freeman GJ, Kuchroo VK, Sharpe AH. PD-L1 regulates the development, maintenance, and function of induced regulatory T cells. *J. Exp. Med.* 2009; **206**: 3015–29.
- Koliarakis V, Prados A, Armaka M, Kollias G. The mesenchymal context in inflammation, immunity and cancer. *Nat. Immunol.* 2020; **21**: 974–82.
- Yang J, Liu XX, Fan H *et al.* Extracellular Vesicles Derived from Bone Marrow Mesenchymal Stem Cells Protect against Experimental Colitis via Attenuating Colon Inflammation, Oxidative Stress and Apoptosis. *PLoS ONE* 2015; **10**: e0140551.
- Yu T, Chu S, Liu X *et al.* Extracellular vesicles derived from EphB2-overexpressing bone marrow mesenchymal stem cells ameliorate DSS-induced colitis by modulating immune balance. *Stem Cell Res Ther* 2021; **12**: 181.
- Ma X, Hu Y, Li X *et al.* *Periplaneta americana* Ameliorates Dextran Sulfate Sodium-Induced Ulcerative Colitis in Rats by Keap1/Nrf-2 Activation, Intestinal Barrier Function, and Gut Microbiota Regulation. *Front. Pharmacol.* 2018; **9**: 944.
- Chen Q, Duan X, Xu M *et al.* BMSC-EVs regulate Th17 cell differentiation in UC via H3K27me3. *Mol. Immunol.* 2020; **118**: 191–200.
- Zhu F, Li H, Liu Y *et al.* miR-155 antagomir protect against DSS-induced colitis in mice through regulating Th17/Treg cell balance by Jarid2/Wnt/ β -catenin. *Biomed. Pharmacother.* 2020; **126**: 109909.
- Varghese F, Bukhari AB, Malhotra R, De A. IHC Profiler: an open source plugin for the quantitative evaluation and automated scoring of

- immunohistochemistry images of human tissue samples. *PLoS ONE* 2014; **9**: e96801.
- 25 Livak KJ, Schmittgen TD. Analysis of Relative Gene Expression Data Using Real-Time Quantitative PCR and the 2- $\Delta\Delta$ CT Method. *Methods* 2001; **25**: 402–8.
- 26 Xu M, Duan X-Y, Chen Q-Y et al. Effect of compound sophorae decoction on dextran sodium sulfate (DSS)-induced colitis in mice by regulating Th17/Treg cell balance. *Biomed. Pharmacother.* 2019; **109**: 2396–408.
- 27 Anagnostou VK, Brahmer JR. *Cancer Immunotherapy: A Future Paradigm Shift in the Treatment of Non-Small Cell Lung Cancer.* *Clin. Cancer Res.* 2015; **21**: 976–84.
- 28 Zuo D, Tang Q, Fan H et al. Modulation of nuclear factor-kappaB-mediated pro-inflammatory response is associated with exogenous administration of bone marrow-derived mesenchymal stem cells for treatment of experimental colitis. *Mol. Med. Rep.* 2015; **11**: 2741–8.
- 29 Bertha M, Bellaguara E, Kuzel T, Hanauer S. Checkpoint Inhibitor-Induced Colitis: A New Type of Inflammatory Bowel Disease? *ACG Case Rep. J.* 2017; **4**: e112.
- 30 Robertson J, Haas CT, Pele LC et al. Intestinal APCs of the endogenous nanomineral pathway fail to express PD-L1 in Crohn's disease. *Sci. Rep.* 2016; **6**: 26747.
- 31 Tian T, Wang Z, Zhang J. Pathomechanisms of Oxidative Stress in Inflammatory Bowel Disease and Potential Antioxidant Therapies. *Oxid. Med. Cell. Longev.* 2017; **2017**: 4535194.
- 32 Chen Y, Yang B, Ross RP et al. Orally Administered CLA Ameliorates DSS-Induced Colitis in Mice via Intestinal Barrier Improvement, Oxidative Stress Reduction, and Inflammatory Cytokine and Gut Microbiota Modulation. *J. Agric. Food Chem.* 2019; **67**: 13282–98.
- 33 Ren Y, Geng Y, Du Y et al. Polysaccharide of *Hericium erinaceus* attenuates colitis in C57BL/6 mice via regulation of oxidative stress, inflammation-related signaling pathways and modulating the composition of the gut microbiota. *J. Nutr. Biochem.* 2018; **57**: 67–76.
- 34 Canbay A, Feldstein AE, Higuchi H, Werneburg N, Grambihler A, Bronk SF, Gores GJ. Kupffer cell engulfment of apoptotic bodies stimulates death ligand and cytokine expression. *Hepatology* 2003; **38**: 1188–98.
- 35 Dong J, Wang H, Zhao J et al. SEW2871 protects from experimental colitis through reduced epithelial cell apoptosis and improved barrier function in interleukin-10 gene-deficient mice. *Immunol. Res.* 2015; **61**: 303–11.
- 36 Lee YR, Chen M, Pandolfi PP. The functions and regulation of the PTEN tumour suppressor: new modes and prospects. *Nat. Rev. Mol. Cell Biol.* 2018; **19**: 547–62.
- 37 Kim DS, Ko JH, Jeon YD et al. *Ixeris dentata* NAKAI Reduces Clinical Score and HIF-1 Expression in Experimental Colitis in Mice. *Evid. Based Complement. Alternat. Med.* 2013; **2013**: 671281.
- 38 Jung YJ, Isaacs JS, Lee S, Trepel J, Neckers L. IL-1beta-mediated up-regulation of HIF-1alpha via an NFkappaB/COX-2 pathway identifies HIF-1 as a critical link between inflammation and oncogenesis. *FASEB J.* 2003; **17**: 2115–7.
- 39 Ichiyama K, Gonzalez-Martin A, Kim BS et al. The MicroRNA-183-96-182 Cluster Promotes T Helper 17 Cell Pathogenicity by Negatively Regulating Transcription Factor Foxo1 Expression. *Immunity* 2016; **44**: 1284–98.
- 40 Ouyang W, Beckett O, Ma Q, Paik JH, DePinho RA, Li MO. Foxo proteins cooperatively control the differentiation of Foxp3+ regulatory T cells. *Nat. Immunol.* 2010; **11**: 618–27.
- 41 Park JS, Kim YS, Jee YK, Myong NH, Lee KY. Interleukin-8 production in tuberculous pleurisy: role of mesothelial cells stimulated by cytokine network involving tumour necrosis factor-alpha and interleukin-1 beta. *Scand. J. Immunol.* 2003; **57**: 463–9.
- 42 Yamada A, Arakaki R, Saito M, Tsunematsu T, Kudo Y, Ishimaru N. Role of regulatory T cell in the pathogenesis of inflammatory bowel disease. *World J. Gastroenterol.* 2016; **22**: 2195–205.
- 43 Blair PA, Noreña LY, Flores-Borja F, Rawlings DJ, Isenberg DA, Ehrenstein MR, Mauri C. CD19(+)/CD24(hi)/CD38(hi) B cells exhibit regulatory capacity in healthy individuals but are functionally impaired in systemic Lupus Erythematosus patients. *Immunity* 2010; **32**: 129–40.
- 44 Kessel A, Haj T, Peri R, Snir A, Melamed D, Sabo E, Toubi E. Human CD19(+)/CD25(high) B regulatory cells suppress proliferation of CD4 (+) T cells and enhance Foxp3 and CTLA-4 expression in T-regulatory cells. *Autoimmun. Rev.* 2012; **11**: 670–7.
- 45 Nguyen LT, Jacobs J, Mathis D, Benoist C. Where FoxP3-dependent regulatory T cells impinge on the development of inflammatory arthritis. *Arthritis Rheum.* 2007; **56**: 509–20.
- 46 Zhu J, Xu Y, Li Z, Liu S, Fu W, Wei Y. Interleukin-36 β exacerbates DSS-induced acute colitis via inhibiting Foxp3(+) regulatory T cell response and increasing Th2 cell response. *Int. Immunopharmacol.* 2022; **108**: 108762.
- 47 Zhu JF, Xu Y, Zhao J et al. IL-33 Protects Mice against DSS-Induced Chronic Colitis by Increasing Both Regulatory B Cell and Regulatory T Cell Responses as Well as Decreasing Th17 Cell Response. *J. Immunol. Res.* 2018; **2018**: 1827901.
- 48 Nadeem A, Ahmad SF, Al-Harbi NO et al. Bruton's tyrosine kinase inhibitor suppresses imiquimod-induced psoriasis-like inflammation in mice through regulation of IL-23/IL-17A in innate immune cells. *Int. Immunopharmacol.* 2020; **80**: 106215.
- 49 Ahmad SF, Ansari MA, Nadeem A et al. The tyrosine kinase inhibitor tyrphostin AG126 reduces activation of inflammatory cells and increases Foxp3+ regulatory T cells during pathogenesis of rheumatoid arthritis. *Mol. Immunol.* 2016; **78**: 65–78.
- 50 Ansari MA, Nadeem A, Attia SM, Bakheet SA, Raish M, Ahmad SF. Adenosine A2A receptor modulates neuroimmune function through Th17/retinoid-related orphan receptor gamma t (ROR γ t) signaling in a BTBR T+ Itpr3tf/J mouse model of autism. *Cell. Signal.* 2017; **36**: 14–24.

Supporting information

Additional supporting information may be found online in the Supporting Information section at the end of the article.

Table S1. Scoring of disease activity index (DAI).

Table S2. Histological evaluations.

Table S3. Primers used in quantitative real-time PCR reactions.